Health Physics Pergamon Press 1967. Vol. 13, pp. 241–251. Printed in Northern Ireland

INJURY DUE TO ACCIDENTAL HIGH-DOSE EXPOSURE TO 10 MeV ELECTRONS*

LAWRENCE H. LANZL and MARTIN L. ROZENFELD
Department of Radiology and the Argonne Cancer Research Hospital†

and

ALVIN R. TARLOV‡
Department of Medicine and the Argonne Cancer Research Hospital†
The University of Chicago, Chicago, Illinois

(*Received* 25 *March* 1966; *in revised form* 14 *July* 1966)

Abstract—An industrial worker was accidentally exposed to a 10-MeV electron beam from a linear accelerator. Dosimetric information was assembled immediately after the event, and later, through a reconstruction of the accident.

The dose gradient about the primary electron beam was high, giving estimated doses to various parts of the right hand which ranged from 40,000 to 240,000 rad. The interior of the body received doses ranging from 0.2 to 5 rad. These measurements of the internal dose were consistent with estimates made immediately after the accident based on the victim's film badge reading and calculations of bremsstrahlung formation in the skin of the chest from a highly scattered electron beam. This early estimate had provided great confidence that the injured would survive, since the blood-forming tissues would not have been impaired by these dosages. Clinical observations pertaining to the development of skin changes and loss of neurologic function in the hand and leg led to much lower estimates of the dosage received by these extremities than the physical dosimetry later provided.

This case illustrates that the ultimate extent of tissue injury and necrosis can not be as yet anticipated from early clinical observation. The late, or delayed, effects of irradiation eventuated in double amputation 5–6 months after exposure. Experimental data in primates is badly needed to provide a foundation for prognosis and a guide to therapy of injured humans.

INTRODUCTION

ACCIDENTAL human exposures have been occurring since the discovery of ionizing radiation. Their number has increased with the development of accelerators and nuclear reactors during the last few decades. Knowledge gained from previous accidents has usually been extrapolated to newer situations, taking account of quality factor, dose distribution, etc. However, the decisions on the treatment of radiation accident victims must ultimately be based on clinical judgment, since accurate dosimetry is at best difficult and many times impossible to obtain under accident situations.

In a recent accident, clinical judgment, based on the accumulation of previous information, underestimated the severity of late effects. This emphasizes the need for additional information on human tissue reactions to various types of ionizing radiation. The following account describes the reconstruction of this accident and the related dosimetry and clinical observations.

* A report of this paper was presented at the First Symposium on Accelerator Radiation Dosimetry and Experience, which was sponsored by the United States Atomic Energy Commission, at Brookhaven National Laboratory, Upton, Long Island, New York on 3–5 November 1965.

† Operated by the University of Chicago for the United States Atomic Energy Commission.

‡ Career Development Awardee, National Institute of Arthritis and Metabolic Diseases, United States Public Health Service.

In February 1965 an industrial worker was accidentally exposed to an electron beam, when he walked into a room to place an octagonal mold on a conveyor belt near the output port of an operational linear accelerator.

As shown in Fig. 1, the accelerator is mounted so that 10.8-MeV electrons are directed downward after emerging into the air from a vacuum chamber at a height of 75 cm from the floor. The maximum peak electron beam current is 200 mA, and the beam pulse length can be varied from 2 to 10 μsec. The accelerator is capable of being operated with single pulses or with repetition rates up to 180 pulses/sec. The machine is provided with a scanning system for beam spreading which operates at a scanning rate of 5 c/s. The beam cross-section at the exit window of the scanning chamber is 3 $\times$ 26 cm. The beam is scanned across the belt and normal to the direction of the conveyor motion.

The beam spreads rapidly in its downward course due to its intrinsic angular distribution coupled with multiple scattering in the window and air. At 46 cm above the floor it strikes a conveyor belt whose function is to carry industrial products through the beam. A schematic view showing the accelerator in relation to the conveyor belt, radiation labyrinth, and service and control rooms is given in Fig. 2. The conveyor system occupies part of the entryway between the service and accelerator rooms. In order to accommodate this conveyor system the bottom of the door, guarding this entryway, had been sawed off. The worker gained entrance to the accelerator room through the resulting gap without tripping the electrical interlocks. After the accident, the door was redesigned to accommodate the conveyor system without leaving a gap.

This paper will not include further discussion of the cause of this accident since the major

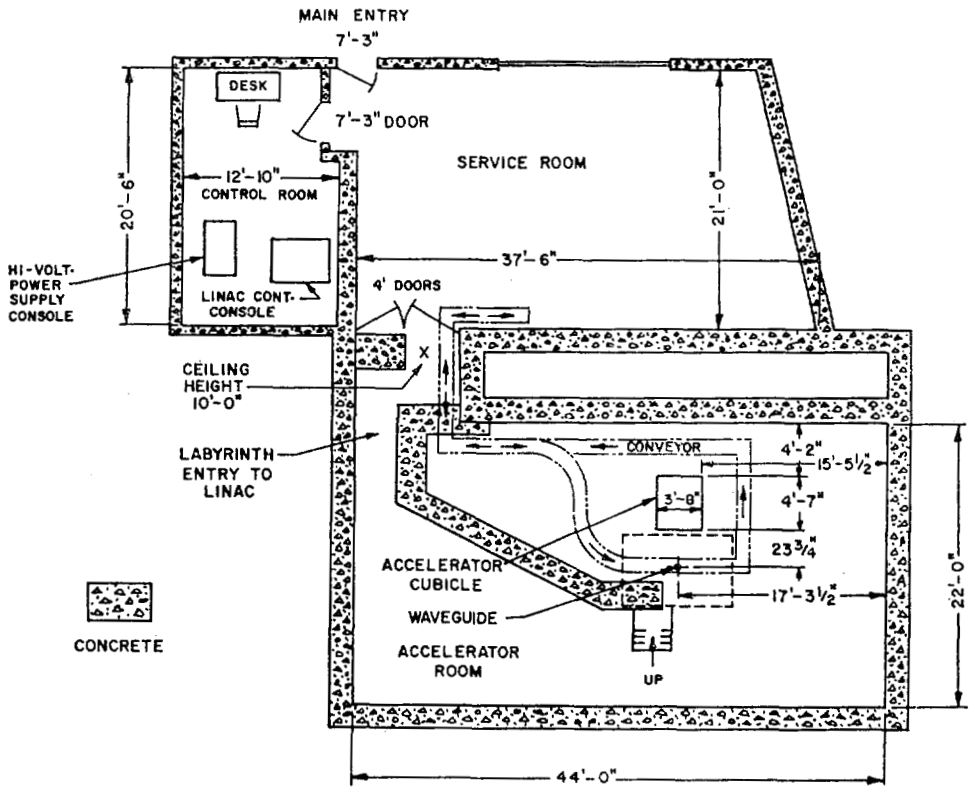

FIG. 2. Schematic drawing of floor plan showing accelerator room, access entryway through radiation labyrinth, service and control rooms. A conveyor belt is capable of transporting industrial products from the service room to the accelerator and then back to the service room.

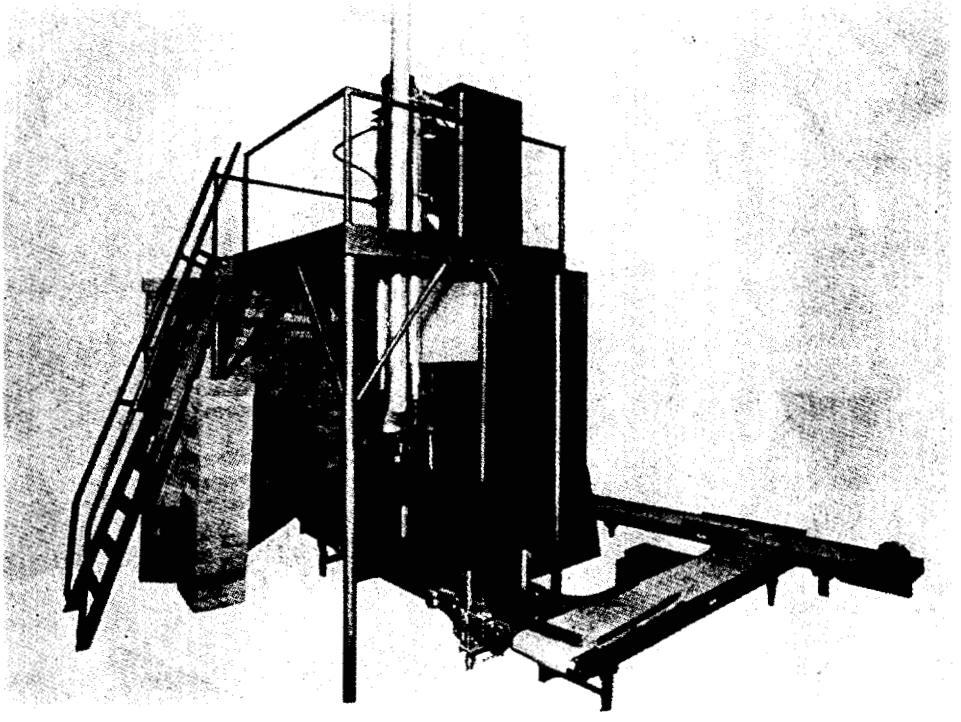

FIG. 1. Over-all view of variable-energy (4–12 MeV) microwave linear accelerator together with conveyor system. The beam is directed downward onto materials placed on the conveyor belt.

emphasis of this work is on its reconstruction and clinical observations of the injured person.

DOSIMETRY

Immediately after the accident, and also throughout a subsequent reconstruction of the event, dosimetric information was assembled to provide information for the physicians which might be useful in making an early prognosis of the extent of radiation damage to various parts of the injured man's body.

Figure 3 is a partial floor plan sketch with isodose rate lines at the floor level. These dose rates are those for the beam current used in the routine production operations of the accelerator.

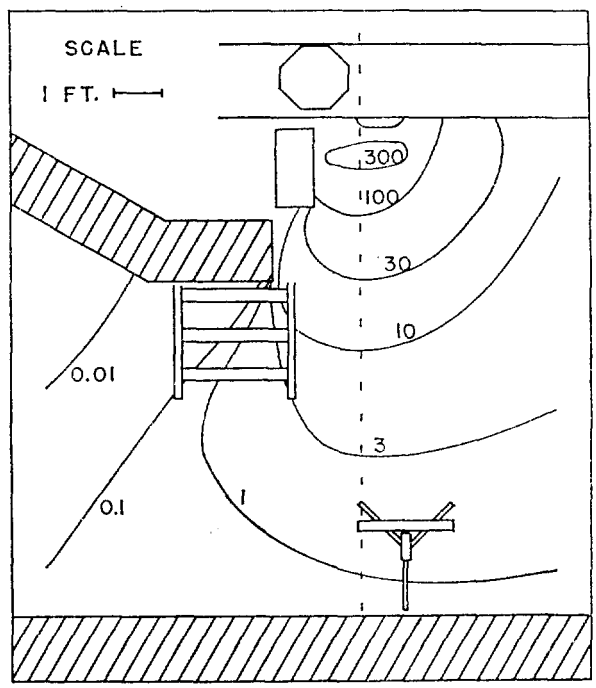

FIG. 3. Schematic drawing of floor plan in the vicinity of the accelerator proper, showing isodose lines at the floor level. The conveyor belt, with the octagonal mold in place, extends across the top of the figure. The vertical dotted line indicates a coordinate system coincident to and extending from the scanning beam location and direction over the conveyor. The rectangular block shown near the conveyor represents the position of a mechanical pump. Parts of the radiation labyrinth are shown in a crossed-line pattern. The location of a ladder (center), a television camera and a bank of lights (bottom) is also indicated. Absorbed dose in rad/sec.

The entranceway through which the worker passed is on the lower left of the figure. The conveyor system runs across the top of the figure. The octagonal mold which the worker carried to the conveyor belt is shown in the position in which he left it. The mold contained an industrial product to be irradiated. The dotted line running vertically in the sketch indicates one axis of a coordinate system set up to facilitate recording of data on the placement of radiation detectors about the accelerator. This axis coincides with the direction of the beam scan over the conveyor.

The dose rate levels were measured by means of lithium fluoride thermoluminescent dosimeters calibrated at the equilibrium depth in a water-like phantom against a collimated beam of cobalt-60 γ-rays. These dosimeters, together with a Controls-for-Radiation reader,* are convenient since they function over several decades, and since the reader can be switched to the proper decade range after heating the dosimeters, but before read out. An intercomparison at several points in the electron field and in the cobalt-60 γ-ray field was made with Sievert-type ionization chambers. It was found that the ratio of response in the electron and gamma radiation fields was the same for both types of dosimeters.

Figure 4 is a sketch of the accelerator, scanning

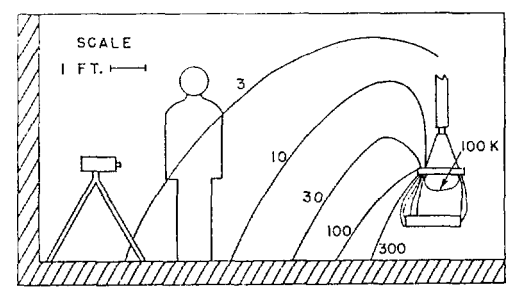

FIG. 4. Isodose lines in a vertical plane as defined by the dotted line in Fig. 3. The end of the accelerator, scanning chamber and conveyor are shown on the right. A television camera and a bank of lights are on the left. The silhouette of the man is shown for scaling purposes only. The isodose lines in the high gradient region just to the left of the accelerator were not labeled for lack of space. Their values are 1K, 3K, 10K and 30K rad/sec respectively.

* Con-Rad TLD System, Model TLD4, Controls for Radiation, Inc., Cambridge, Massachusetts.

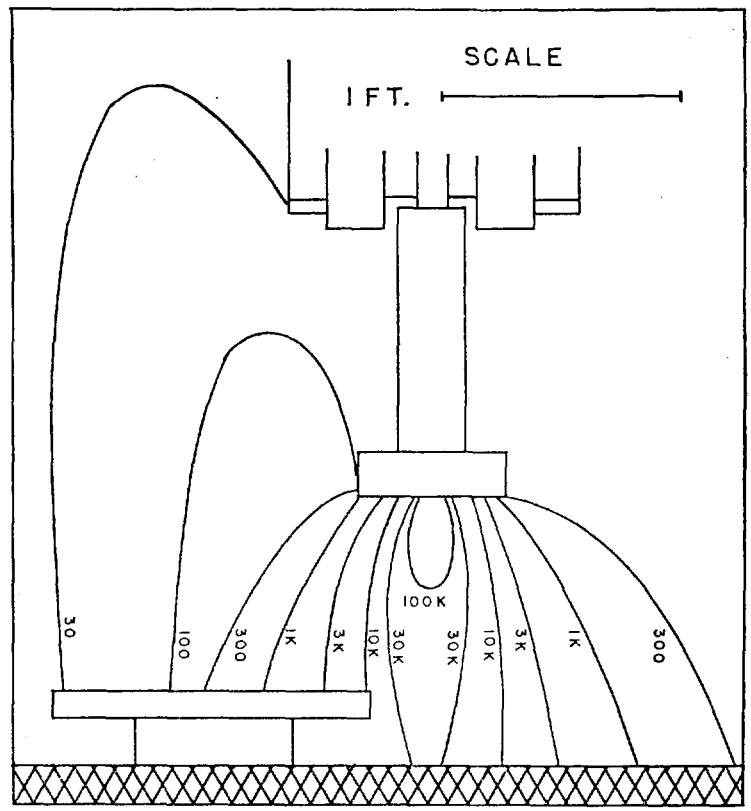

FIG. 5. Isodose lines in a vertical plane at right angles to the dotted line in Fig. 3 and in the mid line of the conveyor belt. The accelerator and the scanning coils are at the top. The scanning chamber is in the center. The cross-hatched lines indicate the conveyor. The mold as positioned by the worker is shown on the lower left. He was facing the belt in the same direction as the reader, so that his left hand was in the 30 rad/sec region and his right hand in the vicinity of the 10K–30K rad/sec region.

chamber, and conveyor on the right side. The left side of the picture shows the location of a television camera and a bank of lights. The figure of the man does not indicate the location of the worker during irradiation, but shows scale only. The isodose rate curves in this figure were determined by thermoluminescent dosimeters in the range of 1000 rad/sec and lower. The higher isodose rate levels around the exit end of the accelerator and conveyor were determined by cobalt-glass dosimetry.* This method involves the change in optical density at 5300 Å following irradiation of the glass. These data were calibrated by means of a cobalt-60 source whose output had previously been measured using chemical and ion chamber dosimetry. The calibration curve for cobalt glass is not quite linear. The value of net optical density change for 1 Mrad is 0.34.

Figure 5 is a more detailed sketch of the equipment and of the isodose rate lines in the radiation field. The view is in a vertical plane normal to that shown in Fig. 4. An edge-on view of the scanning chamber is shown in the center of the picture. The mold is in the position on the lower left, where it was placed during the accident. The conveyor belt extends over the entire bottom of the picture. The conveyor belt was not moving before, during or following the accident. This fact enabled us to determine the location not only of the worker's hands but also

* Dosimeter Glass F-0621, 1.5-mm thickness, Bausch and Lomb Inc., Rochester 2, New York.

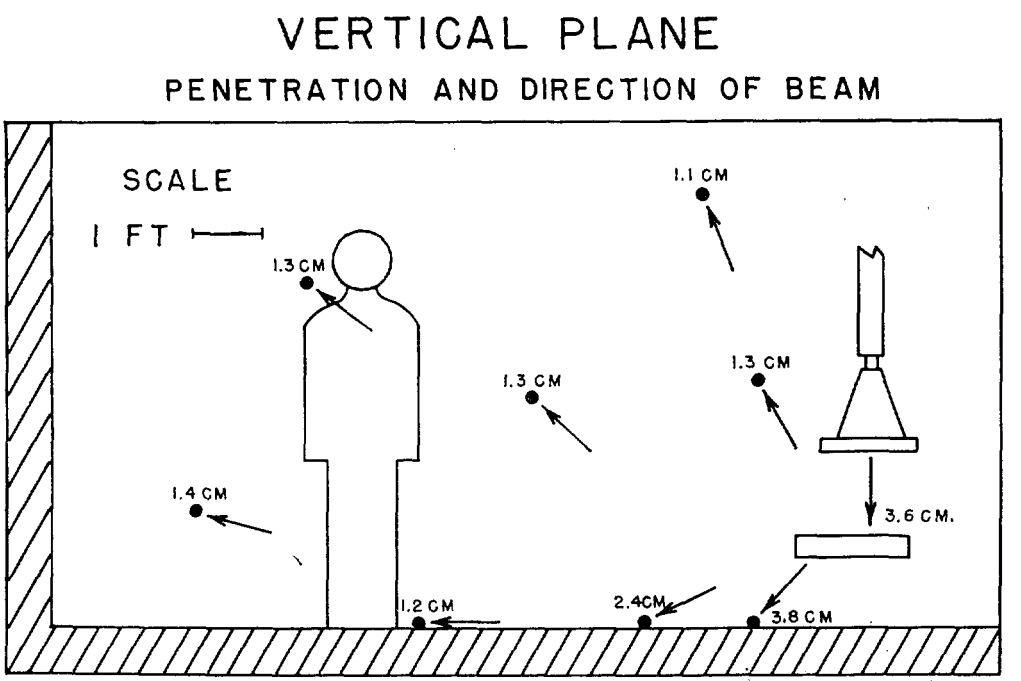

FIG. 6. The direction of the scattered electron beam at various locations in the same plane as Fig. 4 is given by the arrows. The arrow pointing down on the right side of the sketch shows the direction of the primary beam as it leaves the accelerator and scanning chamber and strikes the conveyor belt. The numbers at each arrow location indicate the depth of the 50 per cent dose point of the beam, measured using a tissue-equivalent phantom (see text).

of his body during exposure. It is to be noted that the mold was placed on a brick which was directly on top of the conveyor. The worker's left hand grasped the mold on the left side in the dose region of 30 rad/sec, and the right hand, on the right side, in the dose region of 10 K–30 K rad/sec. The mold was held with the thumb on top of the mold and the fingers curled underneath. Thus, the fingers received some radiation protection from the mold. Of course, when the mold was released by the right hand, the fingers presumably swept through the fringe beam without the benefit of this shielding.

The dose distribution within the body is of prime importance. Such distributions depend on several factors, such as the type of radiation, i.e. X-rays, γ-rays, electrons, neutrons, etc; energies of the radiation; and the collimation of the radiation beam as contrasted with open sources having various degrees of isotropy.

To establish direction, degree of isotropy, and degree of penetration (i.e. energy) of the electrons, a simple circular phantom of unit density was used with Adlux* film as a detector. This film was chosen because of its low sensitivity. The phantom was constructed of a stack of 8-cm diameter Masonite disks with circular pieces of film placed between the disks. The results of the measurements are shown in Fig. 6. The crescent shape of the blackening on all the films indicates a high order of unidirectionality of the scattered electrons, the source of scatter being the conveyor. The direction (see Fig. 6) of the scattered electrons at various locations is indicated by the arrows. This view is in the same plane as shown in Fig. 4. The arrow pointing down on the right side of the sketch shows the direction of the primary beam as it leaves the accelerator and scanning chamber and strikes the conveyor belt. The numbers at each arrow indicate the depth of the 50 per cent dose level of the beam.

* Photo Products Department, E. I. Du Pont de Nemours and Co., Wilmington 98, Delaware.

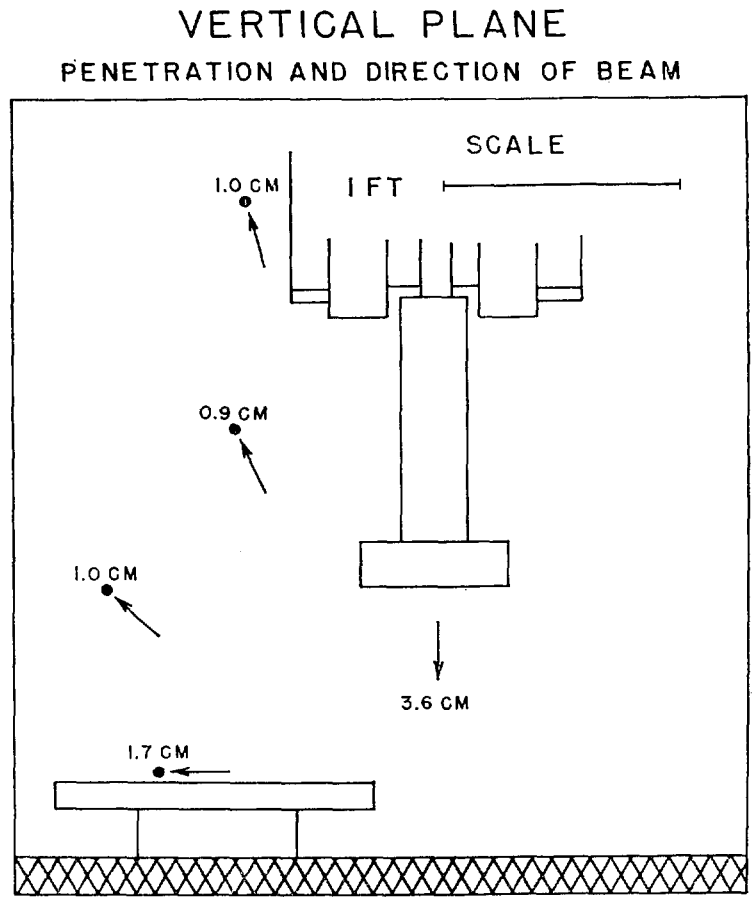

FIG. 7. Direction of the scattered electron beam at various locations in the same plane as Fig. 5. The arrow pointing down in the lower center of the figure shows the direction of the primary beam as it leaves the scanning chamber. The conveyor belt and the mold position are shown at the bottom of the sketch.

The 50 per cent dose depth of the primary beam was determined by a rectangular shaped unit-density phantom in which 3-mm-thick window glass was embedded in a plane parallel to the primary beam. The discoloration of the window glass served as the radiation detector. The extremely high output precluded the use of film in this primary beam study. The high absorption of the glass itself resulted in a 50 per cent dose depth of 3.6 cm, which is slightly less than the highest 50 per cent dose depth of 3.8 cm as measured with film in the Masonite phantom. It is interesting to note that the depth of penetration, averaging about 1.2 cm, does not differ much at any of the locations several feet away from the conveyor, even though the total scattering angle varies from 90 to 180°. The 50 per cent dose depth of 1.2 cm indicates an effective electron energy of about 2.5 MeV in the scattered beam.

Figure 7 shows the direction of the scattered electron beam and depth of the 50 per cent dose at various locations in the same plane as Fig. 5. The arrow pointing downward in the lower center of the figure shows the direction of the primary beam as it leaves the scanning chamber. The conveyor belt and the mold position are shown at the bottom of the sketch.

The above measurements were made in the vicinity of the accelerator, without the presence of a whole-body phantom. These studies were followed by a determination of the location of

the worker during the greatest exposure to his body. This location was then used in conjunction with body and extremity phantoms to measure the absorbed dose received by the worker in various areas.

An attempt was made to duplicate as closely as possible the actions of the worker when the accident occurred. The information used included statements of the worker himself and of his co-workers who, however, were not eye witnesses; the location of equipment and facilities (especially the mold), the vacuum pump, the scanning chamber and shielding walls at the time of the accident; the location of radiation burns on the patient, and re-enactment sequences.[1] Detailed radiation field patterns were correlated with the radiation burns. These detailed patterns were determined by the radiation browning of 61 cm × 61 cm × 3 mm window glass placed at locations corresponding to the worker's right hand and forearm, right foot and right leg. Figure 8 is a photograph with two of these pieces of glass in place after irradiation. The upper part of the photograph shows the scanning chamber together with the browning of the glass in the region of the right forearm. The conveyor belt is seen in the center of the picture. At the bottom, the estimated position of the worker's foot is outlined on the browned glass pattern. It is to be noted that the toe region of the right foot was partially protected by the conveyor belt side support. This area of protection and foot location was directly verifiable by the location and extent of the actual radiation burns on the foot and leg of the worker. X-ray films could have been used in principle for some of these detailed pattern studies, but window glass has the advantage of not requiring development.

Figure 9 is a photograph of a person in the position of the injured worker. A rigid heterogeneous phantom[2]* was placed in a position approximating as closely as possible the position of the trunk and head of person in Fig. 9. The phantom was clothed in a laboratory coat and eye glasses, as was the injured worker.

A number of exposures of the phantom were made to determine dose levels on the surface and in the interior of the trunk and head. Figure 10 is a photograph of an exposed piece of Adlux film placed at the level of the abdomen. The darkened edge indicated a high surface exposure on the worker's front right side, with little radiation to the left rear portion of the body. It is especially important to determine radiation-free skin areas in cases where heterotopic skin grafts are indicated. The clear area in the center of films such as that illustrated by Fig. 10 indicates that a minimal dose was received by the internal organs of the abdomen, thorax and head.

Thermoluminescent dosimeters were also used in and on the phantom. To determine the time during which the worker was in the radiation area, a series of exposures was made with a personnel film badge and thermoluminescent dosimeters located on the phantom at the position of the worker's film badge (left chest) during the accident. A plot of the dose vs. the net optical density readings behind the open window, aluminum, and two thicknesses of silver filters is given in Fig. 11. The net optical density readings of the accident exposure are shown as a series of four horizontal lines in the figure. Averaging these readings gives a dose to the film badge, i.e. to the skin, of 310 rad. This dose, together with the usual operating current of the accelerator as monitored, but not recorded, by the current pickup from an aluminum plate placed below the conveyor belt, indicates that the worker was in the radiation field for 8.5 sec. In other words, assuming that the usual operating current of the linear accelerator did obtain during the accident, it would require that the accelerator be on for 8.5 sec to give a blackening on the chest film badge corresponding to 310 rad. It is evident that the worker received most of this dose while in the position indicated in Fig. 9 since it should take a maximum of only a few seconds to walk into and out of the high dose region as shown in Figs. 3 and 4. Thus adequate dosimetric information was obtained with a stationary phantom at a single position instead of a phantom system that could integrate the dose received while moving toward and away from the beam.

* The phantom systems were purchased with funds from the Damon Runyon Memorial Fund, New York, and the Cancer Research Foundation, The University of Chicago.

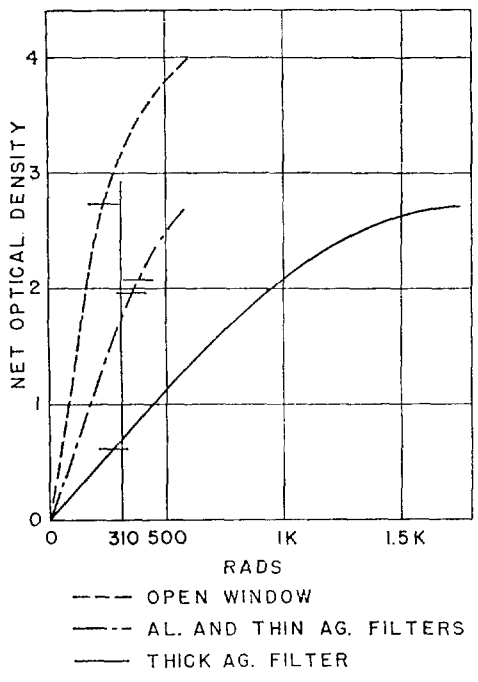

FIG. 11. Calibration curve of personnel film badge. Net optical density is plotted against dose. The net optical density readings of the

in Fig. 9. The toes on the foot received an estimated 11,000 rad, the instep 29,000 rad and the arch of the foot 300 rad. These figures were determined by assuming the right foot was in the indicated position for 8.5 sec. It is estimated that the dose to the anterior surface of the distal portion of the right leg was of the order of 29,000 rad and that the dose diminished progressively toward the right knee. Unfortunately a leg phantom was not available to us for a more detailed study.

A forearm and hand paraffin phantom containing a skeleton was located as shown in Fig. 12. This phantom did not articulate so that the position of the fingers is approximated and lacks some shielding by the mold. Dosimeters were placed at various parts on the surface of the hand and between the fingers. The dose gradient about the primary electron beam was high as shown earlier, giving an estimated dose to the thumb of 240,000 rad and to the little finger region of 42,000 rad. These estimates are based on the assumption made from an interview with the worker, that the hand was in the beam for the same length of time as the trunk of the body, which was determined to be 8.5 sec. It is possible, however, that his hand

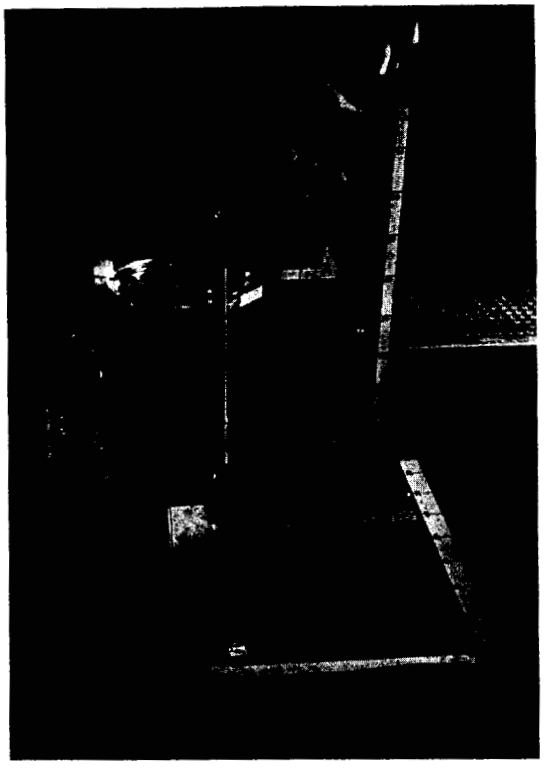

FIG. 8. Photograph of scanning chamber, top, conveyor with mold, center, together with window glass showing beam browning in the region of the right forearm position. At the bottom, the outline of the worker's foot position is shown on a second piece of radiation-browned glass.

FIG. 9. Photograph of model in region of greatest radiation exposure. Note that the right hand is on the fringe of the direct beam and the right foot is slightly forward of the left foot.

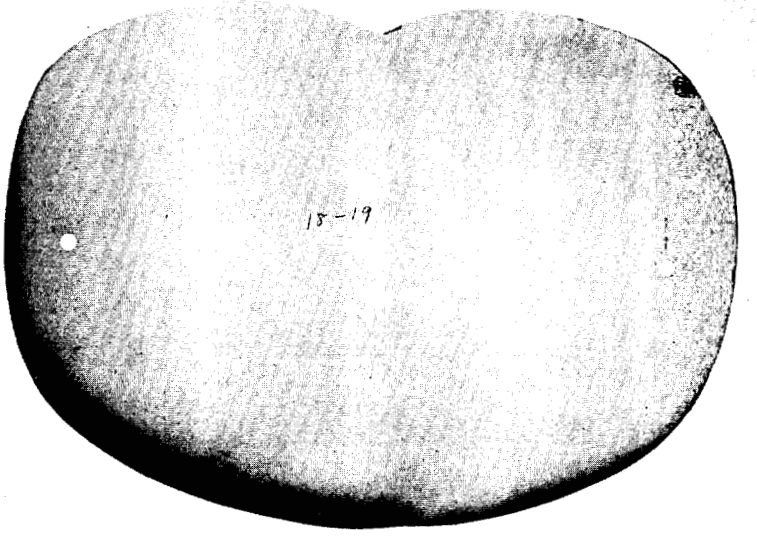

FIG. 10. Photograph of Adlux film exposured in phantom to electrons at abdominal level. Note film blackening on edge of right front portion with little internal blackening. For scaling purposes the distance between the centers of the two registration circles, shown in white above, is 25.7 cm.

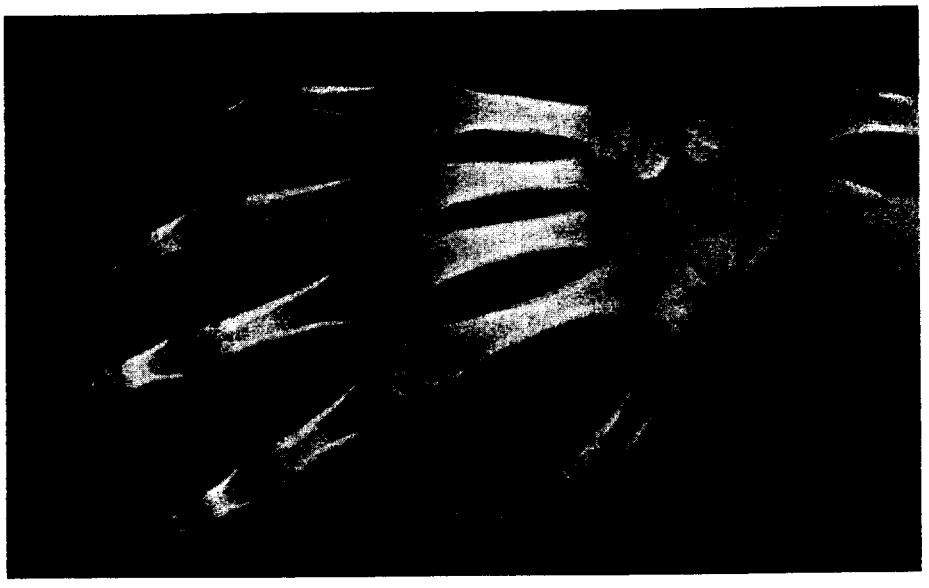

FIG. 19. Clinical impression from radiograph of the right hand taken on 26 May 1965 shows extensive osteoporosis of the third, fourth and fifth digits and aseptic necrosis of the first digit and part of second digit due to destruction of blood supply.

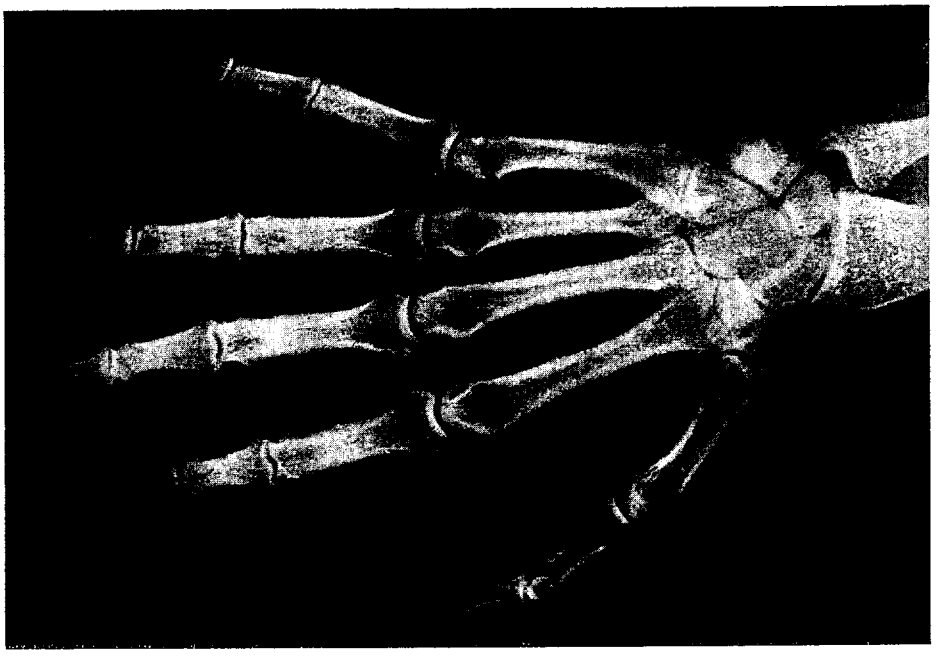

FIG. 20. Radiography of the right hand of an average male of the same age as the injured worker presented for comparison with Fig. 19.

Table 1. Dose determination based on phantom measurements for an 8.5-sec exposure

Location	Dose (rad)
Right hand, thumb	240,000
fifth digit	42,000
Right foot, instep	29,000
toes	11,000
arch	300
Eyes, with glasses	43
Anterior and right surface of trunk, range	240–325
Posterior and left surface of trunk	1.4–6
Interior of trunk	0.22–4.9

Figures 13 and 14* show the hand at 11.00 a.m. on 19 February (Day 2). There is erythema over the entire hand and the distal third of the forearm. Swelling was most marked about the thumb, beginning at its base and extending backward to the mid-forearm. Later that day, the patient described a burning sensation at the wrist between the thumb and index finger. On the following day, he complained that this thumb felt cold. On Day 4, 21 February, two bullous lesions, 3 × 4 cm and 2 × 2 cm, appeared on the dorsal surface of the right thumb, extending to the index finger. Medication was necessary to control pain. Although movement of the fingers was limited by swelling, there appeared to be no neurological deficit on Day 5.

Figures 15 and 16 are photographs taken on Day 7. By Day 8 the swelling had extended to the axilla and involved the anterior axillary folds and anterior chest wall. All sensation in the thumb had vanished, except for pain on movement at the metacarpal phalangeal joint. Bullae formed over the thenar and hypothenar eminences and extended into the palm. The skin over the thenar eminence turned white and the tissue below had a bluish hue. The right leg continued to show only mild erythema laterally.

On Day 9 the bullous lesions over the base of the thumb and palm continued to enlarge and weep serous gelatinous material. The enlargement, but not the weeping, ceased by Day 11 (see Figs. 17 and 18). Edema appeared to be on the decrease, but still extended to the axilla.

Pain in the hand and forearm became severe and was only partially relieved by medication. On Day 12 Dr. SEAN MULLAN† performed a percutaneous cervical electric chordotomy,[3] selectively removing pain from the right upper extremity but leaving tactile sensation and proprioception intact. This procedure, developed by Dr. MULLAN at the University of Chicago, results in temporary loss of pain sensation which subsequently returns in 2 to 12 weeks, depending on the magnitude of the current used and the duration of its application.

Approximately 2 weeks after the accident, the bullous lesions ruptured. Healthy granulation tissue began to grow in from the edges of the lesions, and although it seemed certain that the thumb would have to be amputated, there was hope that the hand and forearm could be saved. This was prior to collection and analysis of the extensive information on dosimetry. However, over the next few months progressive necrosis of the deep structures, muscle, tendon, nerve and bone, slowly developed. Blood vessels underwent complete deterioration. Infection with pyocyaneous organisms supervened late in the course. Figure 19 is a radiograph of the worker's right hand taken on 26 May 1965. A normal right hand of an individual of the same age is shown in Fig. 20. Dr. NELS STRANDJORD‡ reported marked soft tissue swelling of the second, third and fourth digits with destruction in areas of the soft tissues and webbing between the fingers. There is also some air in the soft tissues, particularly at the third and fourth digit. The density of the bones of the first digit including the trapezium appear to be normal. The bone density of the second metacarpal is also within essentially normal limits. The remainder of the bones of the hand and the carpal bones are extremely osteoporotic. There is destruction of the cartilage joint spaces

* We are indebted to Dr. ROBERT WALSH for the photographs.

† Professor, Department of Surgery, The University of Chicago, Chicago, Illinois.

‡ Present address: Chairman, Department of Radiology, University of Kansas Medical Center, Kansas City, Kansas.

at the metacarpal, phalangeal joints of the second, third, fourth and fifth digits. There is also destruction of a styloid process of the radius. Dr. STRANDJORD, knowing the thumb to be necrotic as well as an area over the second metacarpal, explained the appearance of the hand to show extreme osteoporosis of disuse of the third, fourth and fifth digits and the carpal bones with the first digit in particular retaining its normal density because it is not viable and has lost its blood supply. Amputation just above the elbow was performed on 6 July, 138 days after exposure.

The delayed tissue response and the necrosis occurring after radiation injury are well illustrated by the course of events in the right foot and leg. Erythema of the anterolateral surface of the leg was present on the day of exposure, but remained stationary for twenty days before the skin broke down. Similarly, the foot appeared completely normal until Day 25, when small vesicles appeared about the nail beds. Generalized erythema of the foot appeared on Day 30, with breakdown of the skin on Day 35 (see Fig. 21, Day 70). Neuromuscular function was intact. Severe pain was treated effectively with another percutaneous cervical chordotomy aimed at the pain fibers from the lower extremity. After 3 months of observation and surface cleansing, surgical debridement was begun. Repeated discouragement was experienced as tissues that appeared to be viable one week became necrotic the next. Slow, but progressive loss of structure and loss of function of the deeper tissues followed, necessitating amputation just above the knee on 24 August, 6 months after exposure.

It should be pointed out that the time of onset of tissue injury is related directly to the dose. In general, the higher the dose, the sooner signs of injury will occur.[4]

The low radiation dose to the trunk of the body which had been determined by dosimetric measurements, was confirmed by the clinical fact that the absolute lymphocyte count, normal on admission, remained normal throughout the entire illness. An early and sustained polymorphonuclear leukocytosis was relatively constant, with a total white count of approximately 18,000 per ml^3 persisting until after amputation. Anemia, thought to be due to chronic and severe inflammation, developed after 2 months and was sustained until after amputation.

CONCLUDING REMARKS

This case re-emphasizes that the ultimate extent of tissue injury and necrosis can not be anticipated from early clinical observation alone. The late effects of irradiation eventuated in the necessity for double amputation 5–6 months after exposure. Based on hindsight much of the severely debilitating (physical and psychological) experience of that 6-month period could have been averted by early amputation. Judgements in that regard might be facilitated in some future accidents where extremities are exposed (1) if it were possible to establish dose levels and distribution promptly, with a small range of uncertainty, and (2) if experiments in primates relating dosimetry to eventual tissue damage were available.

Information which might have been helpful in this situation was not available in the extensive literature on serious radiation accidents. Some of this literature involves mixed neutron- and gamma-radiations of rather uniform distribution over the entire body.[5,6] Other reports have dealt with radiations such as low-energy X-rays, or electrons with high-gradient distributions which lead to substantial doses to the surfaces of the extremities.[7–10] To a limited extent, these latter reports deal with accidents similar to that described here, but at lower dose levels and with a somewhat less penetrating radiation field to the extemities.

Acknowledgements—We wish to thank the linear accelerator personnel and their firm's officials for their most cooperative help and advice in this study. The calibration of the glass dosimeter by chemical and ion chamber dosimetry was carried out by KEITH CLARK.

REFERENCES

1. R. G. GALLAGHAR, *Radiation Accidents and Emergencies in Medicine, Research and Industry* (Edited by L. H. LANZL, J. H. PINGEL and J. H. RUST) p. 236. Thomas, Springfield, Illinois (1965).
2. S. W. ALDERSON, L. H. LANZL, M. ROLLINS and J. SPIRA, *Am. J. Roentgenol., Radium Therapy Nucl. Med.* **87,** 185 (1962).
3. S. MULLAN, *Postgrad. Med.* **37,** 636 (1965).
4. F. WACHSMANN and A. YIANNAKOPOULOS, *Strahlentherapie* **100,** 428 (1956).

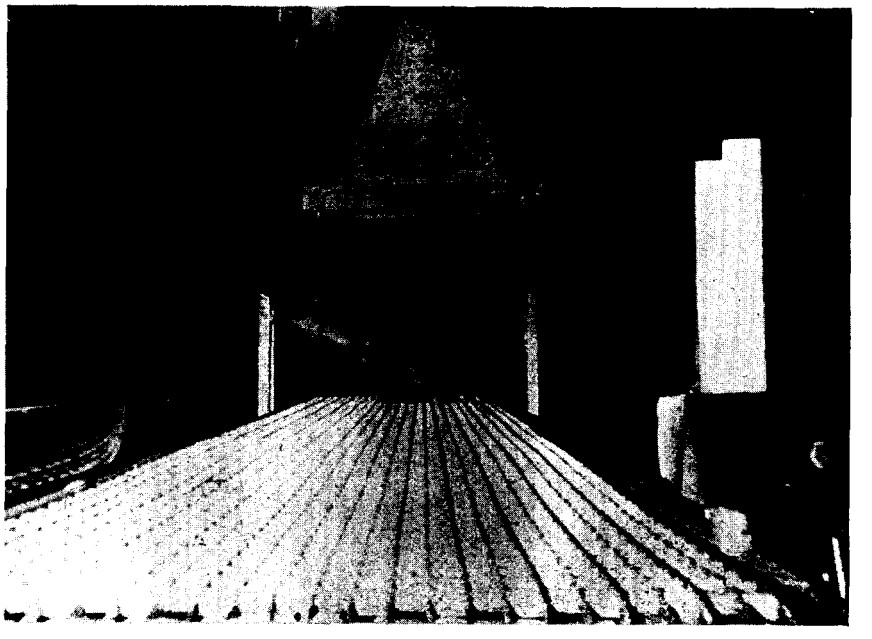

FIG. 12. Photograph of the forearm and hand paraffin phantom containing a skeleton in the location between the scanning chamber and conveyor.

13

14

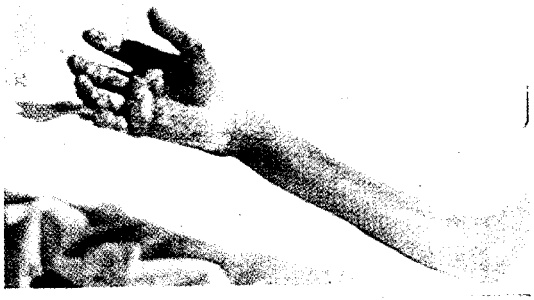

15

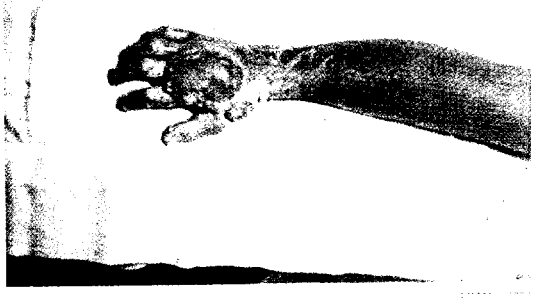

16

17

18

21

FIG. 13. Right hand, 19 February 1965, 11.00 a.m., Day 2.

FIG. 14. Right hand, 19 February 1965, 11.00 a.m., Day 2. There is erythema over the entire hand. Swelling is most marked about the thumb, beginning at the base and extending to the mid-forearm.

FIG. 15. Right hand, 24 February 1965, 11.00 a.m., Day 7. The white material in this and subsequent photographs is from an ointment that was incompletely removed during cleansing before photography. Bullae which formed over the thenar and hypothenar eminences are clearly visible.

FIG. 16. Right hand, 24 February 1965, 11.00 a.m., Day 7.

FIG. 17. Right hand, 28 February 1965, 10.00 a.m., Day 11.

FIG. 18. Right hand, 28 February 1965, 10.00 a.m., Day 11. Enlargement of bullous lesions ceased, but lesions continued to weep serous gelatinous material.

FIG. 21. Right foot, 28 April 1965, Day 70. Generalized erythema of the foot appeared on Day 30. Onset of tissue injury in the foot occurred later than that of hand because of the lower dose to the foot.

5. G. E. Thoma and N. Wald, *J. Occup. Med.* **1,** 421 (1959).
6. J. S. Karas and J. B. Stanbury, *New Engl. J. Med.* **272,** 755 (1965).
7. L. L. Robbins, J. C. Aub, O. Cope, D. G. Cogan, J. L. Langohr, R. W. Cloud and O. E. Merrill, *Radiology* **46,** 1 (1946).
8. R. Grabiger and O. Nehrkorn, *Strahlentherapie* **123,** 132 (1964).
9. R. D. Sweet, *J. Clin. Radiol.* **15,** 55 (1964).
10. J. B. Brown and M. P. Fryer, *Ann. Surg.* **162,** 426 (1965).